



Published in final edited form as:

*Nat Neurosci.* 2007 July ; 10(7): 861–869. doi:10.1038/nn1915.

## A central role for Necl4 (SynCAM4) in Schwann cell–axon interaction and myelination

Ivo Spiegel<sup>1</sup>, Konstantin Adamsky<sup>1</sup>, Yael Eshed<sup>1</sup>, Ron Milo<sup>1</sup>, Offra Sarig–Nadir<sup>1</sup>, Ido Horresh<sup>1</sup>, Steven S. Scherer<sup>2</sup>, Matthew N. Rasband<sup>3</sup>, and Elior Peles<sup>1</sup>

<sup>1</sup>Department of Molecular Cell Biology, The Weizmann Institute of Science, Rehovot 76100, Israel.

<sup>2</sup>Department of Neurology, University of Pennsylvania Medical School, Philadelphia, PA 19104, USA.

<sup>3</sup>Department of Neuroscience, University of Connecticut Health Center, Farmington, CT 06032, USA.

### Abstract

Myelination in the peripheral nervous system requires close contact between Schwann cells and the axon, but the underlying molecular basis remains largely unknown. Here we show that cell adhesion molecules (CAMs) of the Nectin–like (Necl, also known as SynCAM or Cadm) family mediate Schwann cell–axon interaction during myelination. Necl4 is the main Necl expressed by myelinating Schwann cells and is located along the internodes in direct apposition to Necl1, which is localized on axons. Necl4 serves as the glial binding partner for axonal Necl1, and the interaction between these two CAMs mediates Schwann cell adhesion. Furthermore, the disruption of the interaction between Necl1 and Necl4 by their soluble extracellular domains, as well as the expression of a dominant negative Necl4 in Schwann cells, inhibits myelination. These results suggest a critical role for Necl proteins in mediating axon–glia contact during myelination in peripheral nerves.

### INTRODUCTION

Myelination of axons by Schwann cells in the peripheral nervous system (PNS) allows fast and efficient saltatory propagation of action potentials along the nerve. The formation of functional myelinated fibers requires the reciprocal communication between Schwann cells and their associated axons. During development, Schwann cells receive specific axonal signals that control their survival, migration and their differentiation into ensheathing (non–myelinating) or myelinating cells<sup>1</sup>. Although many of the axonal signals that regulate the initial differentiation of Schwann cells are known, the molecular events governing the onset and progression of myelination are much less understood<sup>1</sup>. In the PNS, myelination is regulated by Neuregulin–1 bound to the axonal membrane<sup>2,3</sup>, indicating that Schwann cell–axon contact may be a prerequisite for myelination. Schwann cells express a number of cell adhesion and recognition molecules (CAMs) that could mediate their association with axons. N–cadherin was suggested to mediate the initial growth of Schwann cell processes and their alignment with

---

Address correspondence to: Dr. Elior Peles, Department of Molecular Cell Biology, The Weizmann Institute of Science, Rehovot 76100, Phone: (972) 8–934–4561, Fax: (972) 8–934–4195, peles@weizmann.ac.il.

#### AUTHOR CONTRIBUTIONS

I.S. cloned and constructed all expression constructs and probes, generated and purified antibodies, designed and performed most of the experiments. He was assisted by R.M. in analyzing the myelination data. K.A. performed the cell adhesion assay. O.S.N. and S.S.S. contributed to gene expression analysis, Y.E. to the co–culture experiments, and I.H. to the immunohistochemical analysis. M.N.R. conducted the remyelination experiments. E.P. headed the project and prepared the manuscript.

axons, as well as glia–glia interaction<sup>4</sup>. However, the expression of N–cadherin is downregulated as precursors differentiate into immature Schwann cells, which occurs days prior to myelination<sup>5</sup>. Myelinating Schwann cells also express neurofascin 155 (NF155)<sup>6</sup>, TAG–17 and gliomedin<sup>8</sup>, all of which are important for Schwann cell–axon interactions at and around the nodes of Ranvier, but appear to be dispensable for myelination<sup>8–10</sup>. Two CAMs of the immunoglobulin (Ig) superfamily (Ig–CAMs), L1<sup>11</sup> and myelin–associated glycoprotein (MAG)<sup>12</sup>, were originally suggested to mediate Schwann cell–axon attachments, but further evidence from gene targeting studies demonstrated that neither of these proteins is required to initiate axon–Schwann cell association<sup>13–15</sup>. Hence, although CAMs were implicated in various developmental stages of myelinating Schwann cells<sup>16–18</sup>, the identity of the molecules mediating axon– Schwann cell contact during myelination still remains elusive.

To identify novel cell surface proteins expressed by Schwann cells at the onset of myelination, we recently screened cDNA expression libraries prepared from dbcAMP–treated primary Schwann cells and 3–day old rat sciatic nerve using a signal–sequence trap<sup>19</sup>. Among the large variety of structurally and functionally diverse CAMs and signaling molecules identified in our screen, we isolated members of the Nectin–like (Nectin, also known as SynCAM or Cadm) family. Nectins are a small group of the Ig–CAM superfamily that includes four different members in human and rodents (Nectin1–Nectin4; see also supplementary Table 1 for nomenclature)<sup>20,21</sup>. Nectin1–Nectin4 are type I transmembrane proteins that contain three Ig–like domains in their extracellular region and a short intracellular domain that mediates their interactions with protein 4.1 and PDZ–domain proteins<sup>22–25</sup>. Nectins mediate Ca<sup>2+</sup>–independent cell–adhesion by binding homophilically, as well as heterophilically to other Nectins or their related nectins<sup>26–28</sup>. Based on their tissue distribution and subcellular localization, as well as their interactions with scaffolding proteins, it was proposed that the Nectins play an important role in the organization of the plasma membrane at specific areas of cell–cell contact<sup>21,29</sup>. Nectin2 (SynCAM1) was shown to be present at both the presynaptic and postsynaptic membranes and to induce functional presynaptic differentiation<sup>26,30</sup>. Nectin1 (SynCAM3) was found at various contact sites between neurons, as well as between neurons and astrocytic processes surrounding synapses in the cerebellum, and along myelinated axons in the PNS<sup>27</sup>. In this study, we report that Nectin4 (SynCAM4) mediates Schwann cell–axon interaction necessary for myelination.

## RESULTS

### Nectin proteins in the peripheral nervous system

To examine the expression of Nectins in the PNS we performed *in situ* hybridization of newborn and 7 day–old rats using specific probes for Nectin1–Nectin4 (Fig. 1a). Nectin1, Nectin2 and Nectin4 were clearly detected in dorsal root ganglia. In contrast to the other Nectins, a strong signal of Nectin4 was also detected in Schwann cells located along the nerve. The expression of Nectin4 dramatically increased in myelinating Schwann cells during the first postnatal week, which corresponds to the initial period of active myelination in the PNS. RT–PCR analysis on mRNA isolated from cultured DRG neurons or Schwann cells showed that, while transcripts of all four Nectins could be detected in DRG neurons, cultured Schwann cells express high levels of Nectin4 and low levels of Nectin2, but do not express Nectin1 or Nectin3 (Fig. 1b). Northern blot analysis of sciatic nerve from different postnatal days demonstrated that Nectin4 mRNA expression increases during the first two weeks after birth in a manner that is reminiscent of other myelin–related genes such as Myelin P0 (MPZ; Fig. 1c). Altogether, these results show that members of the Nectin gene family are differentially expressed by neurons and myelinating Schwann cells in peripheral nerves – sensory and motor neurons express Nectin1 and Nectin2<sup>25,31,32</sup>, whereas myelinating Schwann cells mainly express Nectin4.

We generated an antiserum against Necl4 that specifically recognized Necl4 but not Necl1–Necl3, and an antiserum that recognized Necl1 and slightly Necl2, but not Necl3 or Necl4 (Supplementary Fig. 1a). Cultured rat Schwann cells immunostained with these antibodies had strong Necl4-immunoreactivity in their cell membrane and processes, but were Necl1-negative (Fig. 1d). Staining of isolated DRG neurons revealed high levels of Necl1 and weaker levels of Necl4 in the cell soma and along the axons (Fig. 1d). In agreement with these findings, Necl4 but not Necl1 could be immunoprecipitated from cultured rat Schwann cells (Supplementary Fig. 1b), further indicating that it is the major member of this family in Schwann cells.

To examine the expression of Necl4 during myelination, we made use of mixed sensory DRG neuron and Schwann cell cultures, which allows a refined analysis of the process<sup>3,8</sup>. Necl4 was weakly expressed in Schwann cells during the first week in culture, but increased thereafter in Schwann cells that were aligned along axons (Fig. 2a–d). The expression of Necl4 appeared to increase further after the induction of myelination and was particularly high in myelinating Schwann cells labeled for myelin basic protein (MBP) or myelin-associated glycoprotein (MAG) (Fig. 2e–j). These results demonstrate that Necl4 protein is found in myelinating Schwann cells and indicate that its expression is up-regulated by axonal contact and myelination.

### Complementary internodal localization of Necl4 and Necl1

The localization of Necl4 and Necl1 in myelinated nerves was determined using affinity purified antibodies to these proteins in combination with antibodies to various axonal or glial markers (Fig. 3). In teased sciatic nerve fibers from adult rats, Necl4-immunoreactivity was detected along the internodes but was absent from the nodes (Fig. 3a–e). This labeling was specific and was completely abolished by preincubating the antibody with a recombinant protein containing the cytoplasmic tail of Necl4 but not of Necl1 (Supplementary Fig. 2). Double labeling of teased rat sciatic nerve fibers for Necl4 and MAG showed a remarkable co-localization of these proteins in Schmidt–Lanterman incisures (SLI), paranodal loops and all along the adaxonal Schwann cell membrane (apposing the axon) (Fig. 3f–g). At the paranodes, Necl4-immunoreactivity was distinct from Caspr, which labels the axoglial junction<sup>17</sup> (Fig. 3e). In contrast to myelinating Schwann cells, Necl4 was absent from GFAP- and L1-labeled ensheathing non-myelinating Schwann cells<sup>1</sup> (Supplementary Fig. 3). Immunolabeling of rat sciatic nerve for Necl1 and Na<sup>+</sup> channels (Fig. 3h), Caspr (Fig. 3i) or Kv1.2 (Fig. 3j), demonstrated that Necl1 was present along the internodes, including the juxtaparanodal region, but was absent from the nodes and paranodes. Occasionally, Necl1 labeling was also detected in the outermost ring of the SLI (Fig. 3k).

Double immunolabeling of cross sections of sciatic nerves for Necl4 and neurofilament (labels axons) or  $\beta$ -dystroglycan (labels abaxonal Schwann cell membrane) provided further evidence that Necl4 was present at the adaxonal membrane surrounding the axon (Fig. 3i–m). In addition, in ~ 15% of the fibers in the sections, Necl4 was found in an inner, wider ring corresponding to incisures (Fig. 3m). In cross sections, Necl1 was localized to the circumference of the axons (marked by neurofilament staining), indicating that it is localized at the axon–Schwann cell interface (Fig. 3n–o). As summarized in Fig. 3p, these results revealed a complementary localization of Necl4 and Necl1 at the axoglial interface along the internodes.

### Differential binding of Necls to neurons and Schwann cells

To characterize possible interactions between members of the Necl family, we tested whether soluble Fc–fusion proteins containing their extracellular domain could bind to sensory neurons or Schwann cells (Fig. 4a–b). Soluble extracellular domains of Necl1 and Necl3 bound to Schwann cells, whereas no binding was detected with the extracellular domain of Necl2 or

Necl4. In contrast, the extracellular domain of Necl1–Necl4 bound to neurites of cultured DRG neurons (Fig. 4b); Necl4–Fc robustly labeled the axons, Necl2–Fc showed moderate binding, and Necl1–Fc and Necl3–Fc showed very weak binding. These findings are consistent with the idea that Schwann cells express Necl4, which mediates Schwann cell–axon interactions by binding to axonal Necl1.

We next examined whether the binding of Necl1–Fc to Schwann cells and Necl4–Fc to DRG neurites is mediated by their interactions with members of the Necl family. We tested the ability of Fc–fusion proteins containing the extracellular domains of Necl1–Necl4 to bind COS7 cell expressing Necl1 or Necl4 (Supplemental Fig. 4). Necl1–Fc binds to cells expressing Necl1–Necl4, while Necl4–Fc strongly bound to cells expressing Necl1 and Necl4 and weaker to cells expressing Necl2 or Necl3. Neither Necl1–Fc nor Necl4–Fc bound to COS–7 cells expressing other IgCAMs that mediate axon–glial contact, such as contactin, neurofascin, L1, MAG, TAG–1 and Nr–CAM (data not shown). These results support the notion that Necl1 and Necl4 comprise a binding pair in peripheral nerves.

### Necl4 is the glial partner for axonal Necl1

To determine directly whether Necl4 is the Schwann cell binding partner for axonal Necls, we examined the ability of Necl1–Fc to bind to Schwann cells that were transfected with a siRNA designed to knock-down the expression of Necl4. In contrast to cells transfected with a control siRNA, Schwann cells transfected with Necl4–specific siRNA showed reduced binding of Necl1–Fc in proportion to the reduction of Necl4 expression (Fig. 4c). Aggregating Necl1–Fc on the surface of Schwann cells using a secondary antibody to human Fc specifically induced the co–clustering of Necl4 but not of other CAMs such as gliomedin, which was clustered by NF155–Fc (Fig. 4d). In a reciprocal set of experiments, reduction of Necl1 expression in DRG neurons by transfection of siRNA abolished the binding of Necl4–Fc (Fig. 4e). Furthermore, aggregating Necl4–Fc on the surface of DRG neurites specifically induced co–clustering of Necl1 but not of Necl2, Necl4 or other IgCAMs such as the axonal isoform of neurofascin, NF186 (Fig. 4f and data not shown). Altogether, these results demonstrate that Necl4 mediates the binding of axonal Necl1 to Schwann cells and that Necl1 is required for the interaction of Necl4 with the axon.

To determine whether the interaction between Necl1 and Necl4 is sufficient to mediate axon–glial adhesion, we tested the ability of purified Schwann cells to adhere to an otherwise non–adhesive plastic surface coated with Fc fusion proteins containing the extracellular domain of Necl1 (Necl1–Fc) or Necl4 (Necl4–Fc), using human–Fc and laminin as negative and positive controls, respectively (Fig. 5). Schwann cells adhered to and spread on Necl1–Fc and laminin, but not on Necl4–Fc or human Fc. In contrast to the adherence on laminin, efficient adherence of Schwann cells on Necl1–Fc did not require the presence of Ca<sup>2+</sup> ions. Pretreating Necl1–Fc substrates with Necl4–Fc, but not with Necl1–Fc, prior to the addition of the Schwann cells, completely abolished their ability to adhere to Necl1–Fc substrate.

### Disruption of Necl1–Necl4 interaction inhibits myelination

The above results suggest that the trans–interaction between Necl4 and Necl1 mediates Schwann cell–axon adhesion. To determine whether disrupting this interaction affects myelination, we added Necl1–Fc, Necl4–Fc, or Zig1–Fc (Zig1 is a related IgCAM expressed in Schwann cells<sup>19</sup>) to co–cultures of DRG neurons and Schwann cells. Fc–fusions were added prior to the induction of myelination, after Schwann cells had already aligned with axons. The cultures were supplemented with fresh Fc–fusion proteins for an additional 10 days and then fixed and immunolabeled for MBP (Fig. 6a–d). The addition of Necl–Fc fusion proteins resulted in a dramatic reduction (~90% by Necl1–Fc and ~80% by Necl4–Fc, p<0.005) in the number of myelin segments as compared to control–treated (Zig1–Fc) or untreated cultures

(Fig. 6e). In contrast, no effect on myelination was observed using soluble extracellular domain of MAG (Supplementary Fig. 5), indicating that although Necl4 and MAG colocalized in the nerve, they play different roles in PNS myelination. No effect on myelination was also reported for the extracellular domains of other IgCAMs including neurofascin<sup>8,33</sup> and NrCAM<sup>34</sup>, further supporting the specificity of the effect of the Necl proteins. Notably, the addition of Necl-Fc fusion proteins to the culture had no effect on Schwann cell proliferation, as determined by the number of DAPI-labeled nuclei per field of view (Necl1-Fc, 478±39; Necl4-Fc, 438±86; Zig1-Fc, 474±40; no Fc, 461±75; *n*=7), or the percentage of BrdU-incorporated nuclei (Necl1-Fc, 8.3±2.2; Necl4-Fc, 11.2±2.1, Zig1-Fc, 7.4±2.3; no Fc, 10.2±1.9; *n*=7). These results indicate that disruption of the axon-glia interactions mediated by Necl proteins inhibits myelination.

Electron microscopy analysis of the cultures 9 days after the induction of myelination revealed that many axons were ensheathed by Schwann cells in both the hFc control and the Necl4-Fc-treated cultures (Fig. 6f-h). However, while in the control cultures 68% (*n*=87) of the Schwann cell processes wrapped around the axon at least 1.5 turns, in the Necl4-Fc-treated cultures membrane wrapping by Schwann cells was only detected in 12% (*n*=118) of the cases (Fig. 6h-i). Instead, in the Necl4-Fc-treated cultures most (88%) of the Schwann cell processes that contacted an axon surrounded it only once or less. In these cultures we frequently detected Schwann cells sending long membrane-protrusions (occasionally sufficient to make a 1.5 turns around the axon), which failed to wrap around the axon, resulting in a horseshoe configuration (upper scheme in Fig. 6h). This analysis suggests that the Necl proteins are not required for the initial axon-glia contact, but rather for the complete ensheathment by Schwann cells and the transition from the ensheathing stage to myelin wrapping.

#### Inhibition of myelination by a dominant negative Necl4

To further examine the role of Necl4 in myelination, we generated a dominant-negative Necl4, containing its cytoplasmic domain fused to GFP (GFP-Necl4CT; Fig. 7a). A similar mutant was shown to interfere with the function of Necl2 in synapse formation in cultured hippocampal neurons<sup>26</sup>, and would then be expected to disrupt the intracellular interactions of Necl4 with cytoskeletal and signaling components in Schwann cells. As a control for GFP-Necl4CT, we used a GFP fusion protein containing the cytoplasmic domain of neurofascin (GFP-NF155CT), which like Necl4, contains consensus sequences for the binding of PDZ domains<sup>35</sup>, and FERM (4.1-ezrin-radixin-moesin) proteins<sup>36</sup>. Both GFP-Necl4CT and GFP-NF155CT were incorporated into a retrovirus, and 3T3 fibroblasts infected with these retroviruses showed intracellular staining of the fusion protein (Supplemental Fig. 6). The same viral stocks were then used to infect proliferating Schwann cells in dissociated DRG cultures<sup>8</sup>, and myelination was analyzed 18 days later by counting MBP-positive myelin segments (Fig. 7b-d). Cultures infected with viruses encoding for GFP-Necl4CT contained significantly fewer myelinated segments (reduced by ~60-65%; *p*<0.001) than GFP-infected cultures, whereas expression of GFP-NF155CT had no significant effect (Fig. 7e). There were no differences in the number or proliferation of Schwann cells between cultures infected with the different viruses. We thus concluded that ectopic expression of the cytoplasmic domain of Necl4 in Schwann cells specifically inhibits myelination.

#### Soluble Necl4 inhibits remyelination of sciatic nerve

To evaluate the significance of Necl1-Necl4 interactions during myelination *in vivo*, we made use of a PNS remyelination paradigm<sup>37</sup>. In this experimental setting, demyelination is induced by lysolecithin, and is followed by a period of remyelination, which is fundamentally similar to developmental myelination. This model has the advantage that it allows an examination of the effect on myelination of various substances introduced directly into the nerve. Furthermore, it avoids the technical difficulties of working with premyelinated axons of newborn animals

due to the smaller size of their nerves, and the fact that the perineurial barrier has not yet fully formed<sup>38</sup>. We induced a focal demyelinating lesion of sciatic nerves by intraneural injection of lyssolecithin and then injected either Necl4–Fc or hFc fusion proteins directly into the demyelinated site 5 and again at 8 days later, at a time when Schwann cells actively remyelinate the lesion<sup>39</sup>. If Necl4 is indeed required for myelination, then addition of the Necl4–Fc fusion protein should function to inhibit remyelination in this model by competing with endogenous Schwann cell Necl4 for the binding of axonal Necl1. We examined the injection sites at 11 dpi by immunofluorescence labeling for MBP, as a marker for compact myelin and for Na<sup>+</sup> channels, as a marker for nodes of Ranvier. Na<sup>+</sup> channel clustering was used since after remyelination, new myelin segments are shorter, resulting in an increased number of nodes of Ranvier<sup>39</sup>. In both the Necl4–Fc and hFc–injected nerves, we found unaffected regions that had intact myelin sheaths with relatively few nodes of Ranvier (Figs. 8a, region c), as well as remyelinated nerve fibers (Figs. 8a, region f and 8b, region d). Remyelinated regions were clearly identified by reduced MBP immunoreactivity and the frequent occurrence of binary clusters of Na<sup>+</sup> channels (Fig. 8a–b, inset). However, in contrast to the control hFc–injected nerves, in the Necl4–Fc injected nerves we also observed large areas that had relatively few remyelinated axons (Figs. 8b, region e, and 8e). Compared to the remyelinated regions (Figs. 8d,f), these zones had 2–3 fold fewer Na<sup>+</sup> channel clusters (Figs. 8e,g), further indicating that the presence of a soluble extracellular domain of Necl4 in the demyelinated nerve inhibits remyelination.

## DISCUSSION

In the present study we provide evidence that Necl4 (SynCAM4) and Necl1 (SynCAM3) mediate critical interactions between Schwann cells and axons during myelination: **(i)** These two CAMs are expressed on apposed cell membranes along the internode of myelinated axons, i.e., Schwann cells express Necl4 and axons express Necl1. **(ii)** Axonal contact increases the expression of Necl4 in Schwann cells, especially at the onset of myelination. **(iii)** Necl4 is the glial binding partner of axonal Necl1, and is both necessary and sufficient for Necl1 binding. **(iv)** Necl4 and Necl1 can recruit and cluster each other specifically to sites of higher ligand concentration on axons and Schwann cells respectively. **(v)** The interaction between Necl1 and Necl4 mediates Schwann cell adhesion. **(vi)** Interfering with Necl4–Necl1 interaction in myelinated cultures using a soluble ectodomain of either molecule inhibits myelination. **(vii)** Ectopic expression of a dominant negative mutant of Necl4 in Schwann cells markedly reduces myelination. **(viii)** Intraneural injection of a soluble Necl4 protein inhibited remyelination of demyelinated sciatic nerves. Based on these results, we propose that Necl4 and Necl1 mediate the intricate Schwann cell–axon interaction that is required for myelination in the PNS.

Myelinating Schwann cells express several members of the immunoglobulin superfamily, including the major peripheral myelin protein P040 that is essential for the generation of compact myelin, MAG, which is required for the maintenance of myelinated axons, as well as NF1556 and TAG–17 which both are necessary for the local differentiation of the axonal membrane around the nodes of Ranvier<sup>17</sup>. The Necl molecules described here represent a novel axoglial cell–adhesion system in myelinated nerves. In the PNS, this adhesion system consists predominantly of two components, glial Necl4 and axonal Necl1. Adding Necl1–Necl4–Fc fusion proteins to COS cells transfected with Necl1–Necl4 showed that all of them can bind to each other (heterophilically) and to themselves (homophilically). This result extends previous studies showing that Necl1 mediates cell adhesion by binding to itself and to Necl–2, as well as to some of the nectins<sup>27</sup>. In situ hybridization and immunohistochemistry revealed that several members of the Necl family are differentially distributed in the PNS: while Necl4 is mainly found in myelinating Schwann cells, sensory neurons express Necl1, Necl2 and Necl4. Nevertheless, in spite of the presence of these three Necls in DRG neurons, binding of Necl4 to axons requires Necl1, and aggregation of Necl4–Fc on DRG neurons specifically

induced the clustering of Necl1 but not of the other Necls. In the reciprocal experiment, Necl1–Fc, but not Necl2–Fc or Necl4–Fc bound to Necl4 in Schwann cells. These results indicate that trans-binding of Necl1 and Necl4 mediates the interaction between sensory axons and myelinating Schwann cells. The same interaction probably occurs between Schwann cells and the axons of motor neurons, as the latter express Nelcl125:31 and Necl1 was detected in all myelinated axons in the sciatic nerve. Necls are well suited to transverse the 14–20 nm periaxonal space along the internodes, as trans-cellular recognition of Necl1 is mediated by its Ig-like V domain, which generates an antiparallel dimeric structure of the appropriate size<sup>41</sup>.

Schwann cells regulate the molecular composition of the axonal membrane they ensheath, thereby allowing rapid saltatory movement of action potentials along the nerve. The axolemma contains a unique set of cell recognition molecules and cytoskeletal linker proteins at the node of Ranvier, the paranodal junction, the juxtaparanodal region<sup>17</sup>, and as we show here, the internodal region. Immunolabeling of rat sciatic nerve revealed an axonal localization of Necl1 along the internodal membrane. Necl1 was also present at the juxtaparanodal region that is found at the end of each internodal segment, but was completely absent from the paranodal junction and the nodes of Ranvier. In cross sections, Necl1 immunoreactivity was detected at the axonal perimeter, suggesting that it is located at the axolemma. This conclusion is further supported by immuno-electron microscopy analysis recently reported by Kakunaga *et al.*<sup>27</sup> who found that Necl1 was concentrated along the axonal membrane.

In myelinating Schwann cells, Necl4 co-localized with MAG at the periaxonal membrane, as well as in SLIs, the paranodal loops and the inner mesaxon. Analysis of *mag*-deficient mice demonstrates that MAG is required to maintain the normal separation of the axonal and adaxonal Schwann cell membrane, but is not necessary for myelination<sup>16</sup>. In agreement, we found that Necl4–Fc, but not MAG–Fc inhibits myelination of DRG neurons by Schwann cells in culture (Supplementary Fig. 5). Nevertheless, the remarkable co-localization of Necl4 with MAG, along with the ability of Necls to bind cytoskeletal adapter molecules<sup>25,27</sup>, raises the possibility that these two IgCAMs may have some overlapping functions in Schwann cells. In addition to its role in mediating Schwann cell–axon contact, Necl4 may also play a role in the generation of autotypic junctions formed between the myelin lamellae at the Schmidt–Lanterman incisures and paranodal loops<sup>18</sup>. Necl proteins interact with several adapter molecules<sup>25,27</sup> that are present at the incisures and paranodal loops<sup>42,43</sup>, thereby providing a link between membrane adhesion and the enriched actin and spectrin cytoskeleton found at these sites<sup>44</sup>. Schwann cells appear to interact with axons at all developmental stages, from the early migration of precursor cells and the alignment of promyelinating Schwann cells along individual axons, to the ensheathment and spiral wrapping of the myelin membrane, as well as the formation of the nodes of Ranvier<sup>16–18</sup>. Our results suggest that Necl proteins mediate axon–glia interaction at the onset of myelination. First, the expression of Necl4 is markedly induced in Schwann cells that have aligned with axons. Second, Necls are located at the axon–glia interface already before the initial MAG<sup>+</sup> ensheathing stage and continue to be present throughout the process of myelination. The concentration of Necl4 at the axoglial interface during early Schwann cells–axon contact (Fig.2) is reminiscent of the asymmetric localization of the polarity proteins Par–3 and Par–6, which were recently suggested to serve as a scaffold that organize CAMs and receptors during the initiation of myelination<sup>45</sup>. Third, interfering with the interaction between Necl4 and Necl1 resulted in inhibition of myelination, but had no effect on either the proliferation or migration of Schwann cells, or on their longitudinal extension and alignment with the axon. Collectively, our results suggest an important role for Necl proteins during the late step of axonal ensheathment and the initiation of myelination. Initial experiments using cultures of mixed cortical cells showed that similar to our findings in the PNS, Necl4–Fc binds to neurons while Necl1–Fc and Necl3–Fc bind to oligodendrocytes (data not shown), suggesting that these molecules may play a similar role in the CNS. The

identification of Necls described here thus represents an important step towards understanding the molecular mechanisms operating in myelination.

## METHODS

### RNA expression analysis

Semi-quantitative RT-PCR was performed using the primers listed in the Supplementary Methods. Total RNA was extracted with TriReagent (Sigma) and cDNA was prepared with the ImProm II Reverse Transcription System (Promega) using PolyT-primers; the amounts of the resulting cDNA were normalized using actin-specific primers. Northern blot analysis of Necl4 was performed as previously described<sup>43</sup> using the same probe that was used for *in situ* hybridizations. In situ hybridization was performed using cRNA probes for Necl1–4 as described in the Supplementary Methods; hybridization was performed at very stringent hybridization-conditions (71.5°C) as previously described<sup>46</sup>.

### Fc-fusion binding, clustering and perturbation experiments

Binding experiments were done by incubating the cells with medium containing different Fc-fusions proteins pre-incubated with anti human Fc-Cy3 as described previously<sup>8</sup>. For clustering experiments, purified DRG-neurons or isolated Schwann cells were incubated with medium containing the respective Fc-fusion protein as described above, washed once and grown for additional 24 hours (DRG) at 37°C or 4 hours (Schwann) before fixing. Fc-perturbation experiments were performed by adding 50 µg ml<sup>-1</sup> purified proteins to the medium of dissociated DRG cultures 2 days before the induction of myelination. Fresh medium containing the Fc-fusion proteins was replaced every second day and the cultures were fixed and stained after 11–12 days of myelination. For illustration of the extent of myelination, pictures of all the MBP-positive segments of a representative slide were overlaid. Myelination was assayed by counting the amount of all MBP-positive segments on the coverslip, which were manually screened in a fluorescence microscope at low magnification using equal settings of the CCD-camera for all coverslips in a given experiment. All MBP-positive segments were photographed and counted with an in house-developed application for MatLab7.0 (MathWorks; the application will be sent upon request). These experiments were repeated two to three times with three to four samples per treatment, and the differences between the means of various treatments were calculated with Welch's test for a two-sample comparison of means with unequal variances between the averages with and without treatment<sup>47</sup>.

### Electron microscopy of myelinating cultures

Cultures grown on coverslips were washed 3 times in Kosnovsky-fixative (2% glutaraldehyde, 3% PFA, 3% sucrose, in 0.1M cacodylate-buffer), fixed in the same fixative for 2.5 hours at room temperature and additional 48 hours at 4°C, washed 4 times in 0.1M cacodylate-buffer and kept at 4°C until further use. Osmification was made in 1% OsO<sub>4</sub>, 0.5% K<sub>2</sub>Cr<sub>2</sub>O<sub>7</sub>, 0.5% K<sub>4</sub>[Fe(CN)<sub>6</sub>]·3H<sub>2</sub>O, 3% Sucrose (in 0.1M cacodylate-buffer) for 2 hours at room temperature before being washed twice in 3% Sucrose (in 0.1M cacodylate-buffer) and three times in DDW. For enhancement, cultures were impregnated with 2% uranyl-acetate for 1 hour. Dehydrated samples were incubated with increasing concentrations of Epon ("hard"). Glass coverslips were removed by treatment for 2 hours in 30% fluoric acid, washed in DDW and dried overnight in an oven. The Epon-blocks of the cultures were then roughly cut into small pieces and re-embedded. Finally, 70–100 nm ultra-thin slices were cut from each block, mounted onto grids and analyzed in a CM-12 Philips electron-microscope equipped with a BioCam CCD-camera.



## Demyelination and intraneural injection of fusion proteins

All experiments involving animals were performed in accordance with the National Institutes of Health Guidelines for the human treatment of animals. Adult Sprague Dawley rats were anesthetized, and the sciatic nerve was exposed. Nerves were injected with 2–3  $\mu\text{l}$  of 1% lysolecithin in sterile Locke's solution (pH 7.4) by using a glass micropipette. To mark the injection sites and observe the filling of each nerve, 0.05% Fast Green (Sigma, St. Louis, MO) was included in the lysolecithin solution. Each incision was then closed and rats were returned to cages for recovery. Five, and then again eight days, after the original lysolecithin injection, rats were anesthetized and each demyelinated site was injected with 3  $\mu\text{l}$  of 3  $\text{mg ml}^{-1}$  human Fc or Ncl4–Fc (3 rats for each fusion protein) diluted in PBS containing 0.05% Fast Green. Each incision was then closed and rats were returned to cages for recovery. Finally, eleven days after the initial injection of lysolecithin the rats were killed and the injected nerves were collected and fixed for 30 min using 4% paraformaldehyde. Nerves were cryoprotected overnight in 20% sucrose, cut in 16  $\mu\text{m}$  thick sections, and immunostained as described previously<sup>48</sup>.

All other methods are described in the Supplementary Methods section.

## Supplementary Material

Refer to Web version on PubMed Central for supplementary material.

## Acknowledgments

We would like to thank Y. Takai for his generous gift of plasmids and antibodies. This work was supported by the NIH grants NS50220 (EP) and NS044916 (MNR), Dr. Miriam and Sheldon G. Adelson Medical Research Foundation's Adelson Program in Neural Repair and Rehabilitation, the US–Israel Binational Science Foundation, and the The Wolgin Prize for Scientific Excellence.

## REFERENCES

1. Jessen KR, Mirsky R. The origin and development of glial cells in peripheral nerves. *Nat Rev Neurosci* 2005;6:671–682. [PubMed: 16136171]
2. Michailov GV, et al. Axonal neuregulin-1 regulates myelin sheath thickness. *Science* 2004;304:700–703. [PubMed: 15044753]
3. Taveggia C, et al. Neuregulin-1 type III determines the ensheathment fate of axons. *Neuron* 2005;47:681–694. [PubMed: 16129398]
4. Wanner IB, Wood PM. N-cadherin mediates axon-aligned process growth and cell-cell interaction in rat Schwann cells. *J Neurosci* 2002;22:4066–4079. [PubMed: 12019326]
5. Wanner IB, et al. Role of N-cadherin in Schwann cell precursors of growing nerves. *Glia* 2006;54:439–459. [PubMed: 16886205]
6. Tait S, et al. An oligodendrocyte cell adhesion molecule at the site of assembly of the paranodal axo-glial junction. *J Cell Biol* 2000;150:657–666. [PubMed: 10931875]
7. Traka M, Dupree JL, Popko B, Karageorgos D. The neuronal adhesion protein TAG-1 is expressed by Schwann cells and oligodendrocytes and is localized to the juxtaparanodal region of myelinated fibers. *J Neurosci* 2002;22:3016–3024. [PubMed: 11943804]
8. Eshed Y, et al. Gliomedin mediates Schwann cell-axon interaction and the molecular assembly of the nodes of Ranvier. *Neuron* 2005;47:215–229. [PubMed: 16039564]
9. Poliak S, et al. Juxtaparanodal clustering of Shaker-like  $\text{K}^+$  channels in myelinated axons depends on Caspr2 and TAG-1. *J Cell Biol* 2003;162:1149–1160. [PubMed: 12963709]
10. Sherman DL, et al. Neurofascins are required to establish axonal domains for saltatory conduction. *Neuron* 2005;48:737–742. [PubMed: 16337912]
11. Seilheimer B, Persohn E, Schachner M. Antibodies to the L1 adhesion molecule inhibit Schwann cell ensheathment of neurons in vitro. *J Cell Biol* 1989;109:3095–3103. [PubMed: 2592417]

12. Owens GC, Boyd CJ, Bunge RP, Salzer JL. Expression of recombinant myelin-associated glycoprotein in primary Schwann cells promotes the initial investment of axons by myelinating Schwann cells. *J Cell Biol* 1990;111:1171–1182. [PubMed: 1697293]
13. Haney CA, et al. Heterophilic binding of L1 on unmyelinated sensory axons mediates Schwann cell adhesion and is required for axonal survival. *J Cell Biol* 1999;146:1173–1184. [PubMed: 1047768]
14. Li C, et al. Myelination in the absence of myelin-associated glycoprotein. *Nature* 1994;369:747–750. [PubMed: 7516497]
15. Montag D, et al. Mice deficient for the myelin-associated glycoprotein show subtle abnormalities in myelin. *Neuron* 1994;13:229–246. [PubMed: 7519026]
16. Bartsch U. Neural CAMS and their role in the development and organization of myelin sheaths. *Front Biosci* 2003;8:d477–d490. [PubMed: 12456309]
17. Poliak S, Peles E. The local differentiation of myelinated axons at nodes of Ranvier. *Nat Rev Neurosci* 2003;4:968–980. [PubMed: 14682359]
18. Spiegel I, Peles E. Cellular junctions of myelinated nerves (Review). *Mol Membr Biol* 2002;19:95–101. [PubMed: 12126235]
19. Spiegel I, et al. Identification of novel cell-adhesion molecules in peripheral nerves using a signal-sequence trap. *Neuron Glia Biol* 2006;2:27–38. [PubMed: 16721426]
20. Biederer T. Bioinformatic characterization of the SynCAM family of immunoglobulin-like domain-containing adhesion molecules. *Genomics* 2006;87:139–150. [PubMed: 16311015]
21. Takai Y, Nakanishi H. Nectin and afadin: novel organizers of intercellular junctions. *J Cell Sci* 2003;116:17–27. [PubMed: 12456712]
22. Fukuhara H, et al. Association of a lung tumor suppressor TSLC1 with MPP3, a human homologue of *Drosophila* tumor suppressor Dlg. *Oncogene* 2003;22:6160–6165. [PubMed: 13679854]
23. Shingai T, et al. Implications of nectin-like molecule-2/IGSF4/RA175/SgIGSF/TSLC1/SynCAM1 in cell-cell adhesion and transmembrane protein localization in epithelial cells. *J Biol Chem* 2003;278:35421–35427. [PubMed: 12826663]
24. Yageta M, et al. Direct association of TSLC1 and DAL-1, two distinct tumor suppressor proteins in lung cancer. *Cancer Res* 2002;62:5129–5133. [PubMed: 12234973]
25. Zhou Y, et al. Nectin-like molecule 1 is a protein 4.1N associated protein and recruits protein 4.1N from cytoplasm to the plasma membrane. *Biochim Biophys Acta* 2005;1669:142–154. [PubMed: 15893517]
26. Biederer T, et al. SynCAM, a synaptic adhesion molecule that drives synapse assembly. *Science* 2002;297:1525–1531. [PubMed: 12202822]
27. Kakunaga S, et al. Nectin-like molecule-1/TSL1/SynCAM3: a neural tissue-specific immunoglobulin-like cell-cell adhesion molecule localizing at non-junctional contact sites of presynaptic nerve terminals, axons and glia cell processes. *J Cell Sci* 2005;118:1267–1277. [PubMed: 15741237]
28. Williams YN, et al. Cell adhesion and prostate tumor-suppressor activity of TSL2/IGSF4C, an immunoglobulin superfamily molecule homologous to TSLC1/IGSF4. *Oncogene* 2006;25:1446–1453. [PubMed: 16261159]
29. Irie K, Shimizu K, Sakisaka T, Ikeda W, Takai Y. Roles and modes of action of nectins in cell-cell adhesion. *Semin Cell Dev Biol* 2004;15:643–656. [PubMed: 15561584]
30. Sara Y, et al. Selective capability of SynCAM and neuroligin for functional synapse assembly. *J Neurosci* 2005;25:260–270. [PubMed: 15634790]
31. Fujita E, Urase K, Soyama A, Kourouki Y, Momoi T. Distribution of RA175/TSLC1/SynCAM, a member of the immunoglobulin superfamily, in the developing nervous system. *Brain Res Dev Brain Res* 2005;154:199–209.
32. Ohta Y, et al. Spatiotemporal patterns of expression of IGSF4 in developing mouse nervous system. *Brain Res Dev Brain Res* 2005;156:23–31.
33. Koticha D, et al. Neurofascin interactions play a critical role in clustering sodium channels, ankyrin G and beta IV spectrin at peripheral nodes of Ranvier. *Dev Biol* 2006;293:1–12. [PubMed: 16566914]
34. Lustig M, et al. Nr-CAM and neurofascin interactions regulate ankyrin G and sodium channel clustering at the node of Ranvier. *Curr Biol* 2001;11:1864–1869. [PubMed: 11728309]

35. Koroll M, Rathjen FG, Volkmer H. The neural cell recognition molecule neurofascin interacts with syntenin-1 but not with syntenin-2, both of which reveal self-associating activity. *J Biol Chem* 2001;276:10646–10654. [PubMed: 11152476]
36. Gunn-Moore FJ, et al. A functional FERM domain binding motif in neurofascin. *Mol Cell Neurosci* 2006;33:441–446. [PubMed: 17045809]
37. Hall SM, Gregson NA. The in vivo and ultrastructural effects of injection of lysophosphatidyl choline into myelinated peripheral nerve fibres of the adult mouse. *J Cell Sci* 1971;9:769–789. [PubMed: 5148016]
38. Thomas, PK.; Olsson, Y. Microscopic anatomy and function of the connective tissue components of peripheral nerve. In: Dyck, PJ.; Thomas, PK.; Lambert, EH.; Bunge, R., editors. *Peripheral neuropathy*. Philadelphia: W. B. Saunders; 1984. p. 97-120.
39. Dugandzija-Novakovic S, Koszowski AG, Levinson SR, Shrager P. Clustering of Na<sup>+</sup> channels and node of Ranvier formation in remyelinating axons. *J Neurosci* 1995;15:492–503. [PubMed: 7823157]
40. Lemke G, Axel R. Isolation and sequence of a cDNA encoding the major structural protein of peripheral myelin. *Cell* 1985;40:501–508. [PubMed: 2578885]
41. Dong X, et al. Crystal structure of the V domain of human Nectin-like molecule-1/Syncam3/Tsll1/Igsf4b, a neural tissue-specific immunoglobulin-like cell-cell adhesion molecule. *J Biol Chem* 2006;281:10610–10617. [PubMed: 16467305]
42. Ohno N, et al. Expression of protein 4.1G in Schwann cells of the peripheral nervous system. *J Neurosci Res* 2006;84:568–577. [PubMed: 16752423]
43. Poliak S, Matlis S, Ullmer C, Scherer SS, Peles E. Distinct claudins and associated PDZ proteins form different autotypic tight junctions in myelinating Schwann cells. *J Cell Biol* 2002;159:361–372. [PubMed: 12403818]
44. Trapp BD, Andrews SB, Wong A, O'Connell M, Griffin JW. Co-localization of the myelin-associated glycoprotein and the microfilament components, F-actin and spectrin, in Schwann cells of myelinated nerve fibres. *J Neurocytol* 1989;18:47–60. [PubMed: 2468742]
45. Chan JR, et al. The polarity protein Par-3 directly interacts with p75NTR to regulate myelination. *Science* 2006;314:832–836. [PubMed: 17082460]
46. Spiegel I, Salomon D, Erne B, Schaeren-Wiemers N, Peles E. Caspr3 and caspr4, two novel members of the caspr family are expressed in the nervous system and interact with PDZ domains. *Mol Cell Neurosci* 2002;20:283–297. [PubMed: 12093160]
47. Sokal, RR.; Rohlf, FJ. *Biometry: The Principles and Practice of Statistics in Biological Research*. W.H. Freeman & Company; 1994.
48. Schafer DP, Bansal R, Hedstrom KL, Pfeiffer SE, Rasband MN. Does paranode formation and maintenance require partitioning of neurofascin 155 into lipid rafts? *J Neurosci* 2004;24:3176–3185. [PubMed: 15056697]

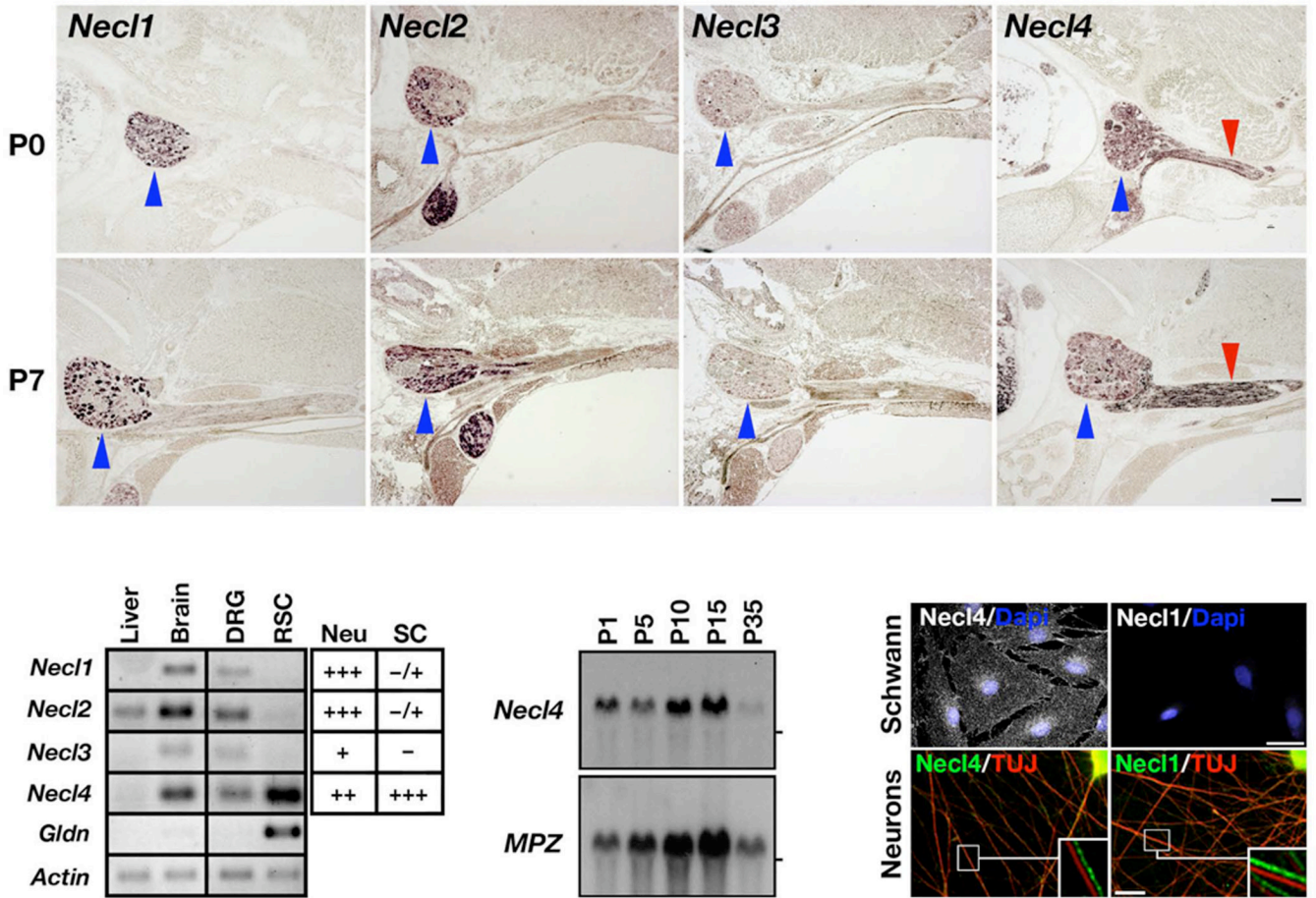


**Figure 1. Differential expression of Necls in the PNS**

(a) In situ hybridization analysis. Cross sections of post-natal day 0 (P0) or P7 rats were hybridized to *Necl1–Necl4* antisense-probes as indicated. Note strong expression of *Necl4* mRNA in the nerve (red arrowheads), and strong expression of *Necl1*, *Necl2*, and *Necl4* mRNA in the DRG (blue arrowheads). (b) RT-PCR analysis. Specific primer sets for *Necl1–Necl4*, gliomedin (*Gldn*), and actin were used to amplify mRNA purified from isolated dorsal root ganglia neurons (DRG) or isolated rat Schwann cells (RSC). Actin and gliomedin were respectively used as controls for genes that are expressed ubiquitously or specifically in Schwann cells. The table summarizes the expression of the Necls in DRG neurons and Schwann cells (based on RT-PCR and in situ hybridization). (c) Northern blot analysis. Blots containing RNA isolated from rat sciatic nerves at the indicated postnatal days were successively hybridized with radiolabeled *Necl4* and P0 cDNAs (*MPZ*). Both mRNAs increased in parallel from P1 to P15. The location of the 18S ribosomal RNA is marked on the right. (d) Immunocytochemistry. Isolated Schwann cells or DRG neurites were immunostained with antibodies to *Necl4*, *Necl1* and  $\beta$ III tubulin (TUJ) as indicated; nuclei were labeled with Dapi (blue). The boxed regions are shown as insets, in which the two fluorescent labels are offset. Scale-bars: (a) 400  $\mu$ m; (d) 30  $\mu$ m.

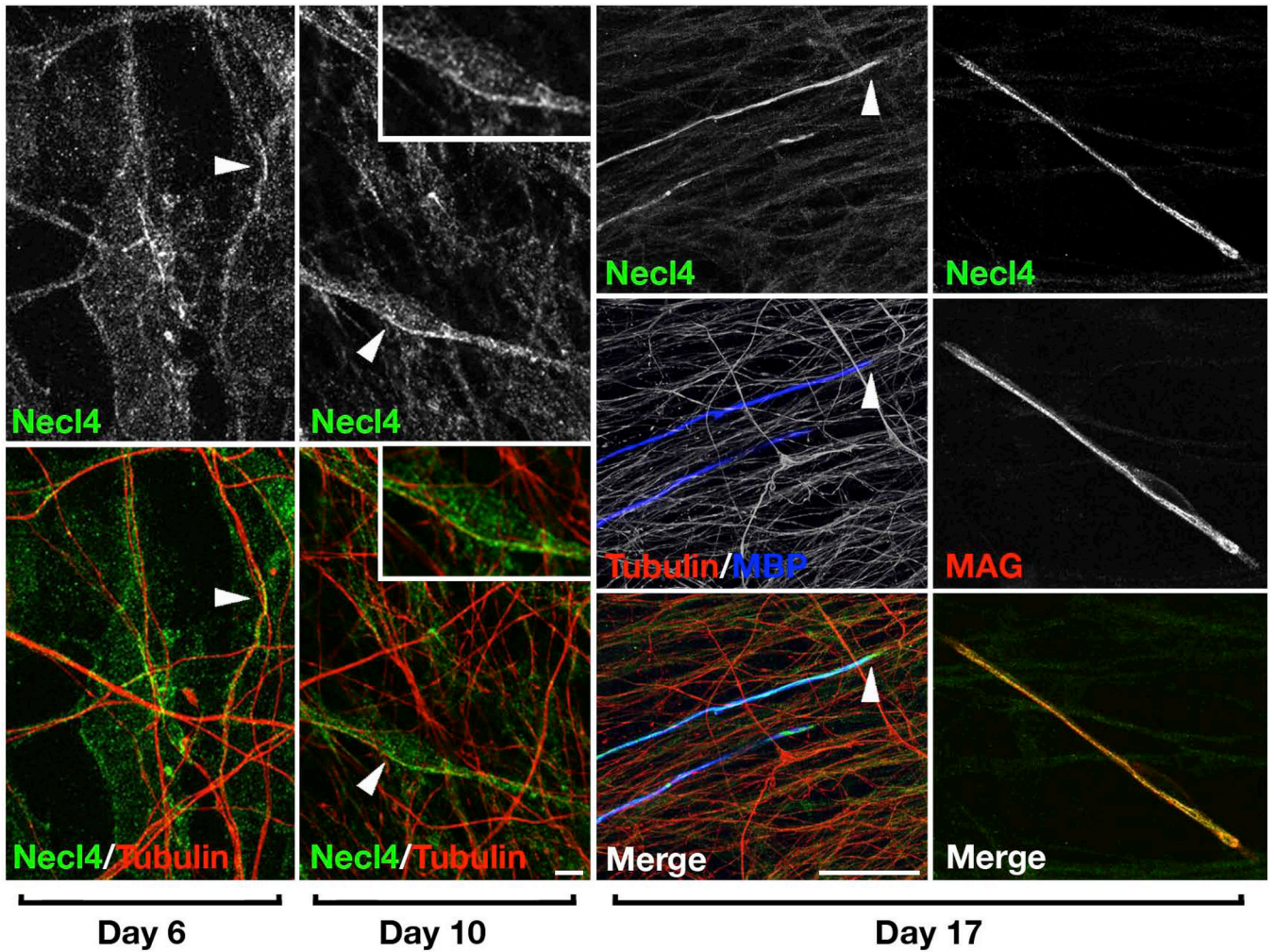


**Figure 2. Axonal contact and myelination are associated with increased expression of Necl4 in Schwann cells**

Cultures of dissociated DRG neurons and Schwann cells were immunostained for Necl4, and  $\beta$ III tubulin, MBP or MAG, 6, 10, or 17 days after plating as indicated; myelination was induced with ascorbic acid at day 10. (a–d) Increased labeling of Necl4 at contact sites between Schwann cells and the axons are marked by arrowheads. Inset in (c–d) show higher magnification images of the areas marked with an arrowhead. (e–j) Myelin basic protein (MBP) and myelin-associated glycoprotein (MAG)-positive myelinating Schwann cells (arrowheads) have intense Necl4-immunoreactivity. Scale bar: (a–d) 10  $\mu$ m; (e–j) 30  $\mu$ m.

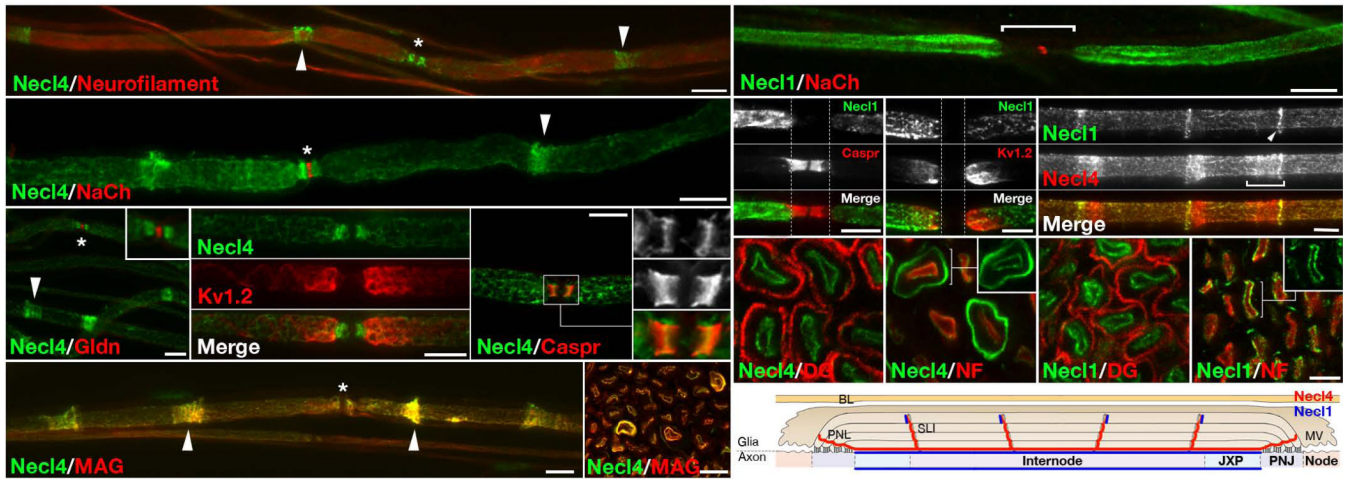


### Figure 3. Necl4 and Necl1 are localized along the internodes

(a–f) Immunofluorescence staining of teased adult rat sciatic nerves for Necl4 and (a) Neurofilament, (b) Na<sup>+</sup> channels (NaCh; to label nodes), (c) Gliomedin (Gldn; to label nodes), (d) Kv1.2 (to label juxtaparanodes), (e) Caspr (to label paranodes), or (f) myelin-associated glycoprotein (MAG), as indicated. (g) Cross sections of adult rat sciatic nerves labeled for Necl4 and MAG. Arrowheads and asterisks mark the incisures and the nodes of Ranvier, respectively. Inset in c shows a higher magnification of the nodal region. Insets in e show a higher magnification of the paranodes labeled for Necl4 (upper), Caspr (middle) or the merged image (lower). (h–k) Teased fibers immunolabeled for Necl1 and (h) Na<sup>+</sup> channels, (i) Caspr, (j) Kv1.2 or (k) Necl4 as indicated. The location of the nodes and paranodes is marked with a horizontal line in h, or with dashed vertical lines in i–j. Note that Necl1 is present along the axonal internodes but is absent from the paranodes or the nodes of Ranvier. The Schmidt–Lanterman incisures, or their outermost ring (arrowhead) is labeled in k. (g–j) Cross sections of adult rat sciatic nerves labeled for Necl4 (l–m) or Necl1 (n–o), together with neurofilament (NF) or dystroglycan (DG), as indicated. (p) A schematic view of a longitudinal section of a myelinated axon, summarizing the localization of Necl4 and Necl1. PNL–Paranodal loops; PNJ–Paranodal junction; JXP–Juxtaparanodal region; SLI–Schmidt–Lanterman incisures; MV–Microvilli; BL–basal lamina. Scale bar: (a–k) 10 μm; (i–o) 5 μm.

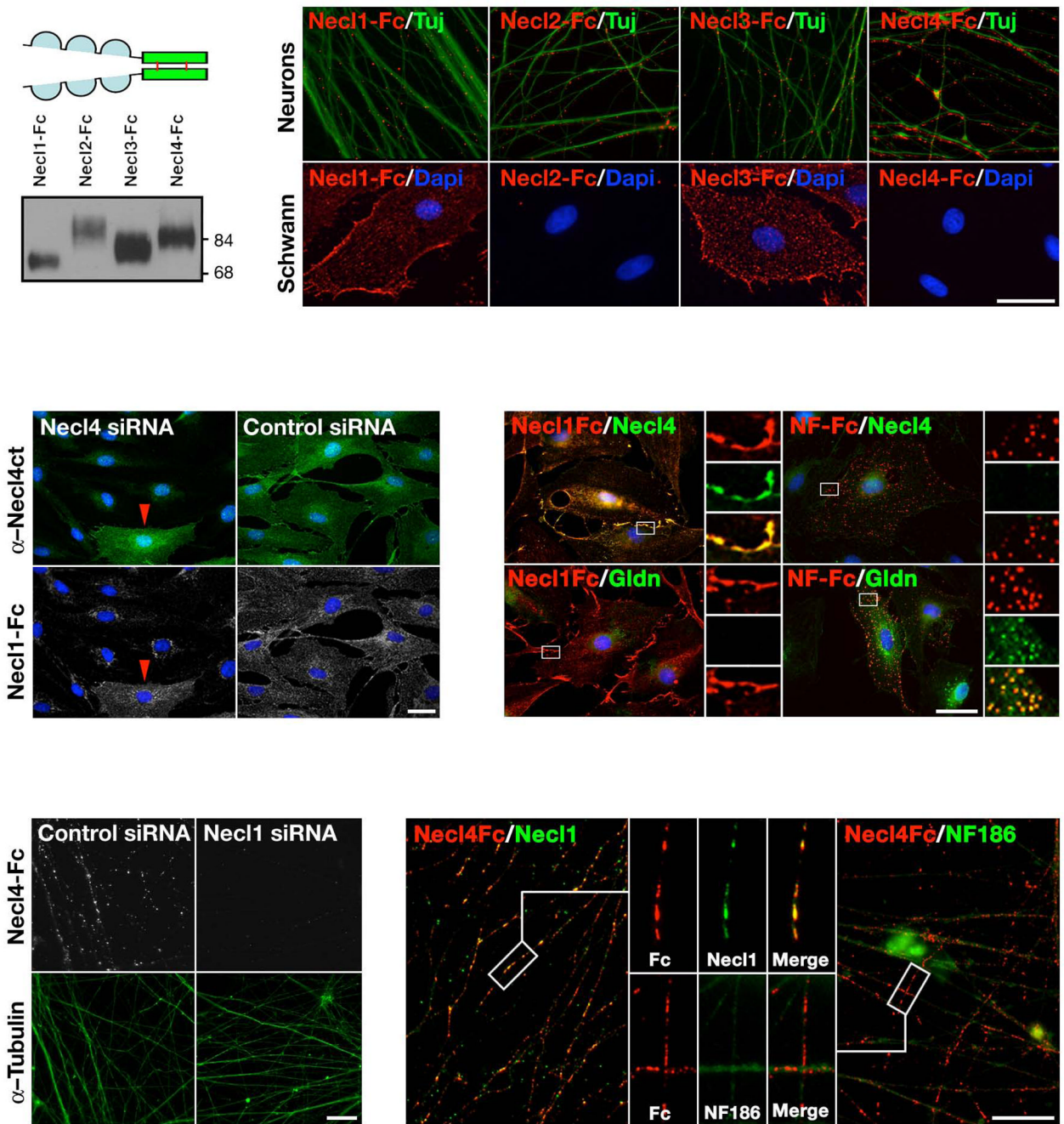


**Figure 4. Necl4 is the glial binding partner for axonal Necl1**

(a) Immunoblot of secreted Fc–fusion proteins containing the extracellular domains of Necl1–Necl4. (b) Differential binding of Necl1–Necl4 to DRG neurons and Schwann cells. Binding of Fc–fusion proteins was detected using a secondary antibody to human Fc, neurites were labeled with an antibody to βIII–tubulin (Tuj), and DAPI was used to label Schwann cell nuclei. The images in the upper panels were shifted to permit better visualization. (c) Down–regulation of Necl4 in Schwann cells abolishes Necl1 binding. Necl1–Fc binding to Schwann cells transfected with a Necl4 or a control siRNA. Binding of Necl1–Fc and the expression of Necl4 (α–Necl4ct) are indicated. (d) Clustering of Necl4 in Schwann cells by Necl1–Fc. Soluble Necl1–Fc or NF155–Fc (NF–Fc) was aggregated on Schwann cells followed by

immunolabeling for Necl4 or gliomedin (green) as indicated. Bound Necl1–Fc co-localized with Necl4. Insets show the separate channels and the merged image of the boxed area. (e) Down-regulation of neuronal Necl1 abolishes Necl4 binding. Binding of Necl4–Fc to DRG neurons transfected with a Necl1 or control siRNA. Neurites were labeled with an antiserum to  $\beta$ III–tubulin in the lower panels. (f) Necl4–Fc induces the clustering of axonal Necl1. Necl4–Fc was aggregated on DRG neurons followed by immunolabeling for Necl1 or the neuronal isoforms of neurofascin (NF186) as indicated. A higher magnification of the boxed region is shown as a single channel or the merged image as indicated. Scale bar: 40  $\mu$ m.



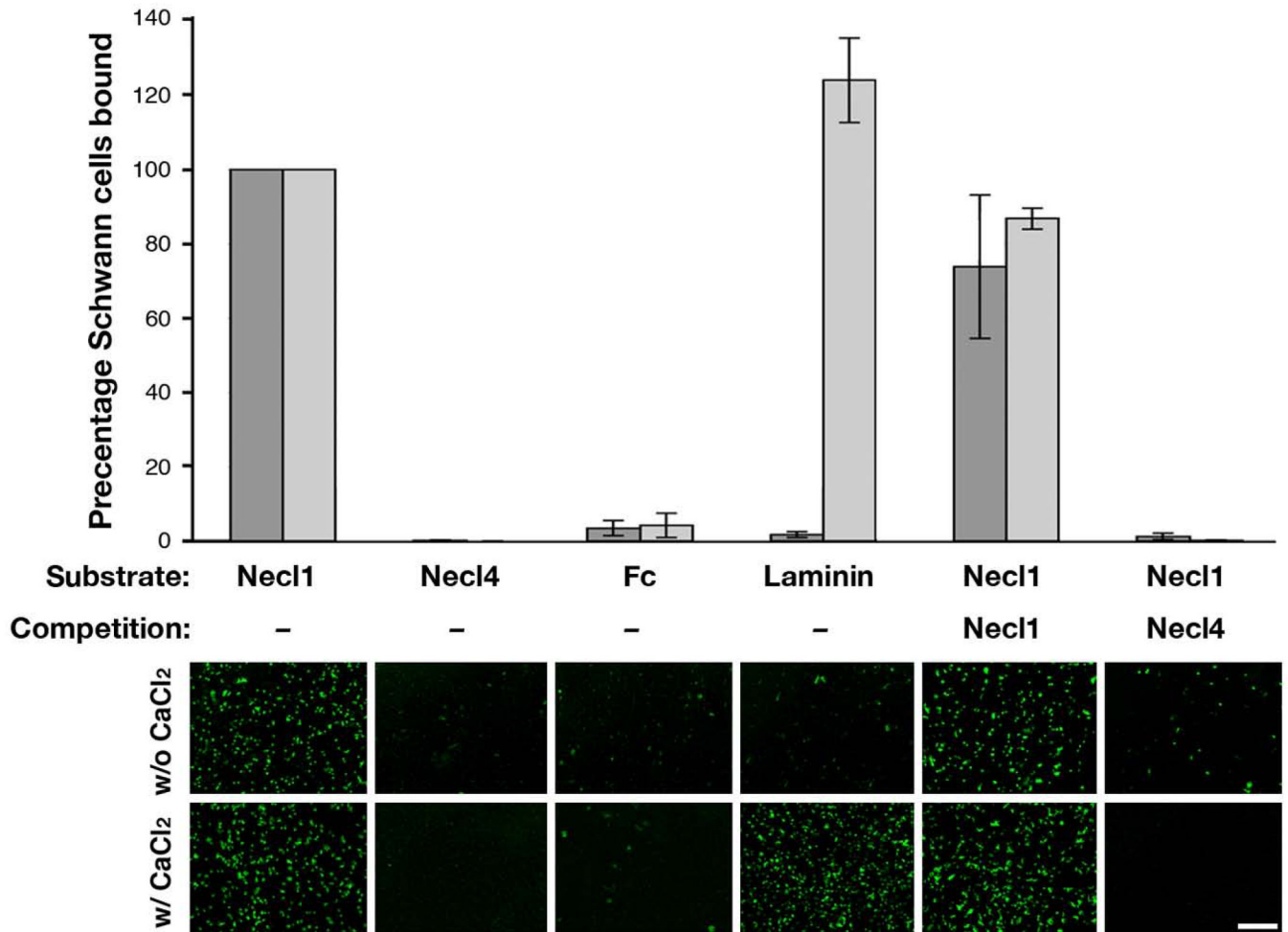


**Figure 5. Necl4–Necl1 interaction mediates Ca<sup>2+</sup>–independent adhesion of Schwann cells**

Schwann cells were added to a plastic dish pre-coated with Fc–fusion proteins containing the extracellular domain of Necl1 (Necl1–Fc) or Necl4 (Necl4–Fc), the Fc region of human IgG (Fc), or laminin. Adherent cells were counted and were compared to the percentage of the cells adhering to Necl1–Fc in the presence (light gray bars) or absence (dark gray bars) of Ca<sup>2+</sup> as indicated. Schwann cells adhered to Necl1–Fc and to laminin, but not to Necl4–Fc. Pretreating Necl1–Fc substrates with Necl4–Fc, but not with Necl1, prior to addition of Schwann cells completely abolished their adhesion. Low–magnification pictures taken from a representative experiment are shown below the graph. Scale bar: 1 mm.

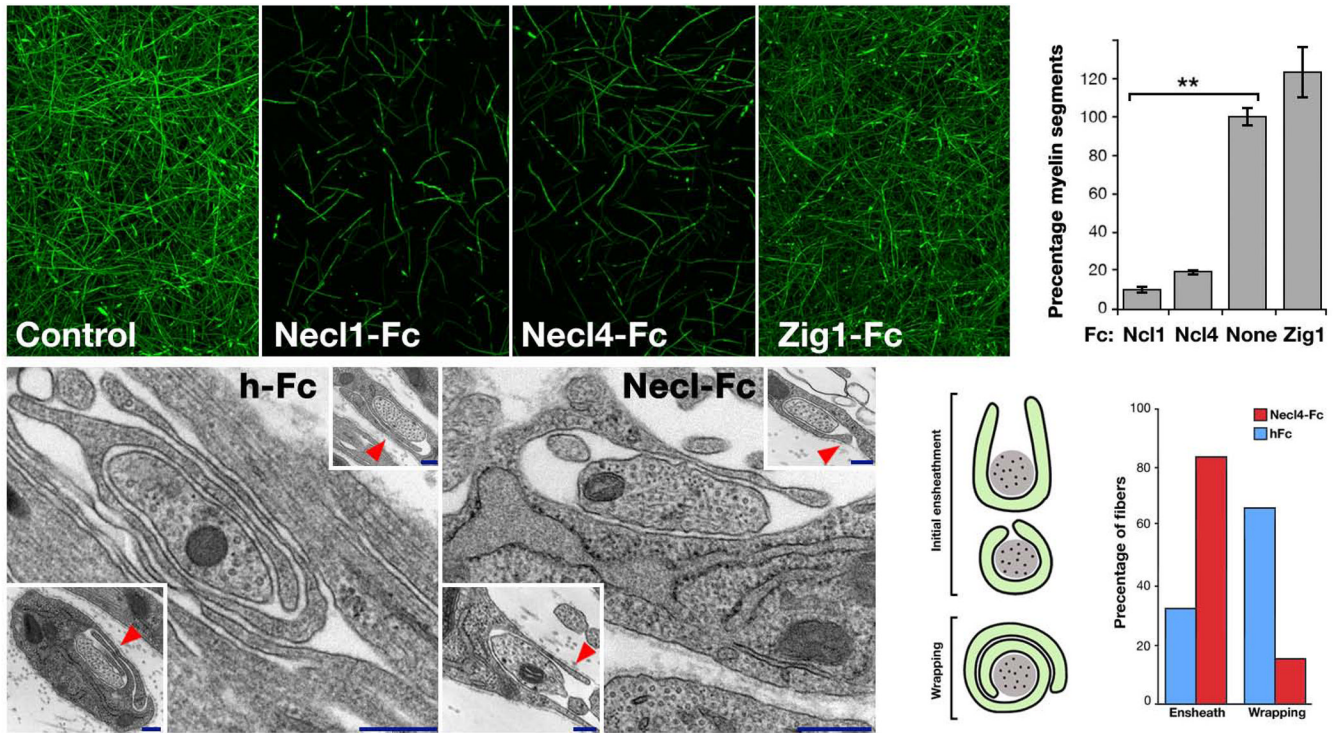


### Figure 6. Necl-mediated axon-glia interaction is required for myelination

Myelinated DRG-cultures were left untreated (a), or grown in the presence of Fc- fusion proteins ( $50 \mu\text{g ml}^{-1}$ ) containing the extracellular domain of Necl1 (Necl1-Fc; b), Necl4 (Necl4-Fc; c) or Zig1 (Zig1-Fc; d) for 10 days, and then immunostained for MBP. The number of MBP-positive segments present in each condition is shown as a percentage of that in the untreated cultures (e). Cultures grown in the presence of Necl-Fc's contained significantly (\*\* $p < 0.005$ ) fewer myelin segments compared to untreated or control-treated (Zig1-Fc) cultures. (f-i) Electron microscopy analysis of myelinating cultures. (f-g) Representative images of 9-day-old DRG and Schwann cells cultures, grown in the presence of human Fc (f) or Necl4-Fc (g). Two additional examples are shown in the insets. Note that while in the control Fc-treated cultures Schwann cell processes already circled 1.5 times around the axon, they fail to do so when the cultures were grown in the presence of Necl4-Fc (red arrowheads). (h) Schematic representation of axons ensheathed (U shape and O shape) and wrapped (1.5 turns and more) by myelinating Schwann cells. (i) The number of ensheathed and wrapped axons in each culture are shown as a percentage of the total sites counted (hFc  $n=87$ ; Necl4-Fc  $n=118$ ). Scale bar: a-d, 100  $\mu\text{m}$ ; g-h, 20 nm.

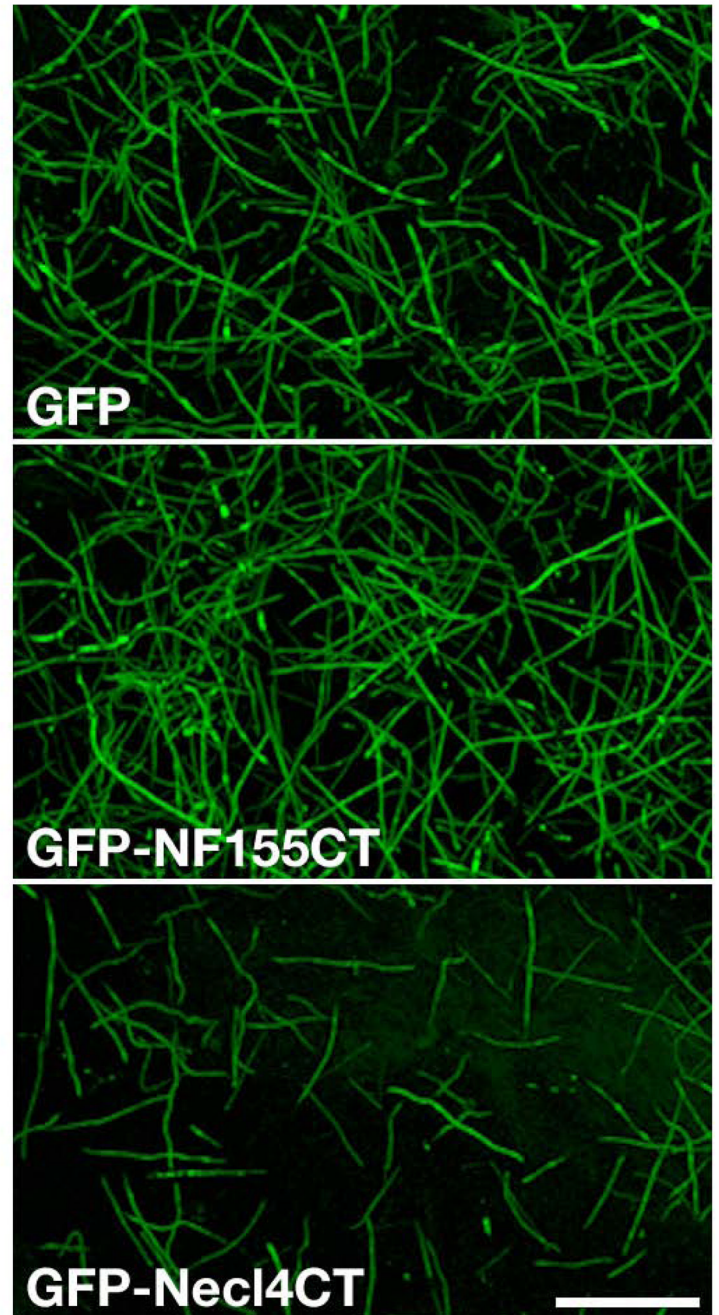
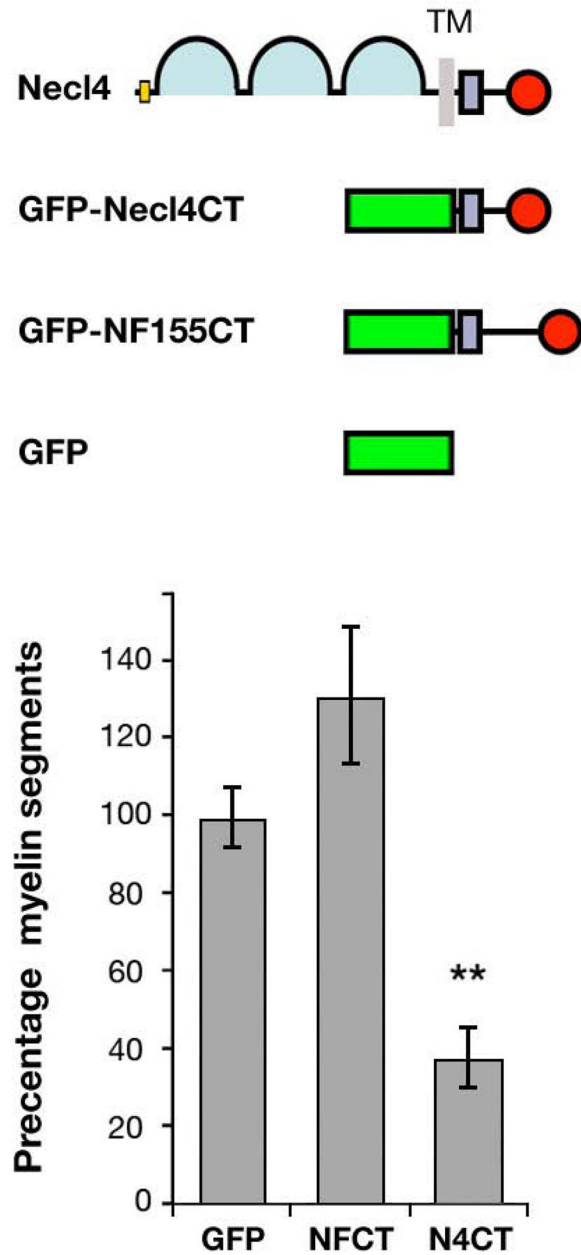


**Figure 7. Expression of a dominant negative Necl4 inhibits myelination**

(a) Schematic presentation of Necl4 and the different constructs used; the cytoplasmic domains of Necl4 and neurofascin 155 contain a 4.1 (purple square) and a PDZ (red circle)–binding sequence. Schwann cells were infected with retroviruses that direct the expression of GFP (b) or a GFP–fusion protein containing the cytoplasmic domain of either neurofascin 155 (GFP–NF155CT) (c) or Necl4 (GFP–Necl4CT) (d). Infected cells were allowed to myelinate sensory DRG axons, and then fixed and immunolabeled for MBP. The extent of myelination was determined by counting the number of MBP–positive segments present in each condition (e). Note that the ectopic expression of GFP–Necl4ct in Schwann cells inhibited myelination by

65% (\*\*  $p < 0.001$ ), while that of the C-terminus of neurofascin had no significant effect, as compared to cultures infected by GFP. Scale bar: 100  $\mu\text{m}$ .

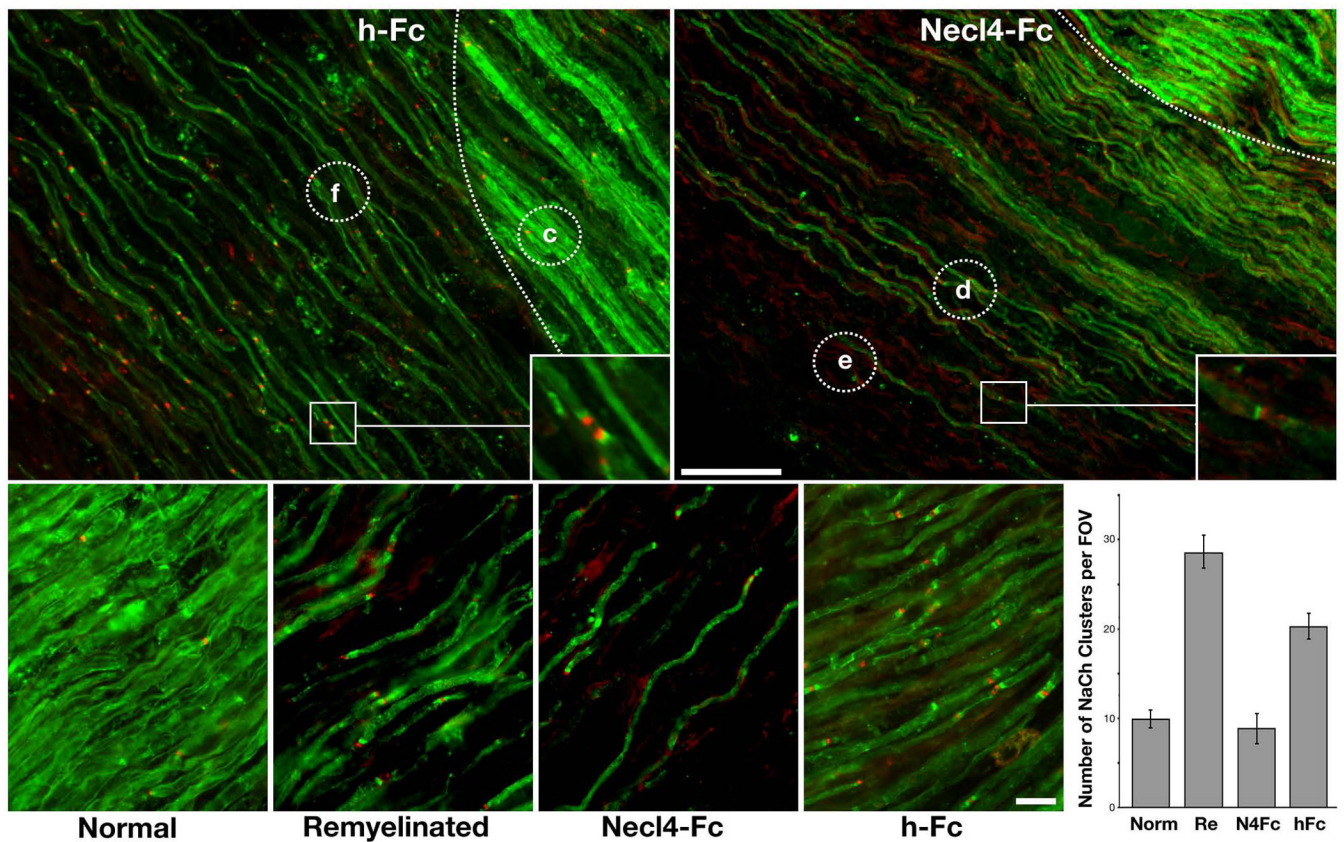


**Figure 8. Necl4-Fc inhibits remyelination *in vivo***

Demyelination of adult rat sciatic nerves was induced by lyssolecithin followed by intraneural injections of human Fc (a) or Necl4-Fc (b) as described in “Material and Methods”. Eleven days post-injection, nerves were collected and longitudinal sections of the injected region were immunostained for MBP (green) and Na<sup>+</sup> channels (red). The border between demyelinated and unaffected region is marked by a dotted line. Insets depict higher magnification images of selected nodes from remyelinated regions, many of which have binary clusters of Na<sup>+</sup> channels. Circles mark the locations of representative regions shown in c–f: unaffected nerve regions (c), remyelinated (d) or inhibited (e) areas in nerves injected with Necl4-Fc, as well as in remyelinated regions of nerves injected with hFc (f). Regions of inhibited remyelination were only detected in the Necl4-Fc and not in the hFc control-injected nerves. (g) The number of Na<sup>+</sup> channel clusters found in the various regions defined in c–f was counted and are shown as an average number (mean±SEM) per field of view (FOV a minimum of 10 FOV were counted for each region). Norm, normal; Re, remyelinated. Scale bar: (a–b) 100 μm; (c–f) 20 μm.